The Interpretation of Spectral Vegetation Indexes

Ranga B. Myneni, Forrest G. Hall, Piers J. Sellers, and Alexander L. Marshak

Abstract—**Empirical studies report several plausible correlations between transforms of spectral reflectance, called vegetation indexes, and parameters descriptive of vegetation leaf area, biomass and physiological functioning. However, most indexes can be generalized to show a derivative of surface reflectance with respect to wavelength. This derivative is a function of the optical properties of leaves and soil particles. In the case of optically dense vegetation, the spectral derivative, and thus the indexes, can be rigorously shown to be indicative of the abundance and activity of the absorbers in the leaves. Therefore, the widely used broad-band red/near-infrared vegetation indexes are a measure of chlorophyll abundance and energy absorption.**

I. Introduction

THE importance of vegetation in studies of global climate and biogeochemical cycles is now well recognized [1]. The physical and physiological parameters of vegetation required in these studies may be obtained from satellite remote sensing. For these reasons, several of the instruments scheduled for the Earth Observing System have land surface studies as major goals [2]. These instruments measure solar radiation reflected by vegetation at certain wavelength intervals. Of these, the broad-band red (0.6–0.7 μ m) and near-infrared (0.75– 1.35 μ m)$ channels have been found to be most valuable in the remote sensing of vegetation.

The measured spectral reflectance data are usually compressed into vegetation indexes. For example, the widely used ratio of near-infrared to red vegetation reflectance is the Simple Ratio index. More than a dozen such indexes are reported in the literature and shown to correlate well with vegetation amount [3], the fraction of absorbed photosynthetically active radiation [4], unstressed vegetation conductance and photosynthetic capacity [5], and seasonal atmospheric carbon dioxide variations [6]. The proliferation and use of vegetation indexes can also be attributed to the ease with which large amounts of satellite data can be processed with minimum effort per pixel, thereby facilitating valuable large spatial- and temporal-scale analyses [7].

While this large body of empirical evidence is impressive and encouraging, a central question remains unanswered: what do vegetation indexes indicate? In other words, what information is encoded in the reflectance spectra of vegetation? It is shown here that the derivative of vegetation reflectance with respect to wavelength, or a related form, is common to all vegetation indexes and is indicative of the abundance and activity of the absorbers (*viz.* pigments, water, nitrogen, etc.). The presented theory provides a physical basis for high-resolution spectral remote sensing of vegetation, by formalizing the relationship between vegetation reflectance spectra and leaf biochemical constituents [8], [9].

Manuscript received April 4, 1994; revised September 29, 1994.

R. B. Myneni is with the University of Maryland, Biospheric Sciences Branch, Mail Code 923, NASA Goddard Space Flight Center, Greenbelt, MD 20771 USA.

F. G. Hall and P. J. Sellers are Biospheric Sciences Branch, Mail Code 923, NASA Goddard Space Flight Center, Greenbelt, MD 20771 USA.

A. L. Marshak is with SSAI, Climate and Radiation Branch, Mail Code 913, NASA Goddard Space Flight Center, Greenbelt, MD 20771 USA.

IEEE Log Number 9408111.

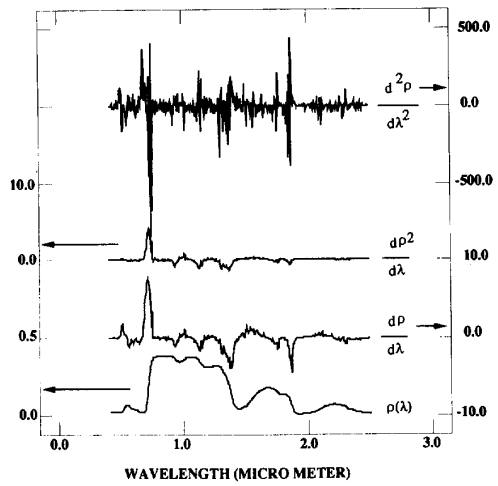

Fig. 1. The reflectance spectrum $\rho(\lambda)$ of a soybean canopy and its spectral derivatives $d\rho/d\lambda$, $d\rho^2/d\lambda$ and $d^2\rho/d\lambda^2$. Solar zenith and azimuth angles are 30° and 225°. The view direction is nadir. The architecture of the canopy is discussed elsewhere [29]. Leaf optical properties were simulated with measured inputs as described in [25]. A radiative transfer model was used to estimate $\rho(\lambda)$ with these inputs [19].

II. Spectral Vegetation Indices

A distinctive feature in the scattering spectrum of a green leaf is the chlorophyll absorption maximum at about 0.69 μm. The lack of absorption in the adjacent near-infrared region (0.85 μm) results in a strong absorption contrast across the 0.65-0.85 μ m wavelength interval (Fig. 1). Vegetation indexes capture this contrast through combinations of broad-band red/near-infrared reflectance.

The atmosphere above and the soil below tend to mask the vegetation signal in a remote measurement. Some vegetation indexes partially correct for these effects and also compensate for the bidirectional geometry of the measurement. Other indexes require pre-processing of data, such as selecting the maximum value in a weekly or monthly composite [10], to unmask the vegetation signal in the measurement. However, most indexes can be expressed in the form $k\rho'$, i.e. a coefficient k times the derivative of surface reflectance ρ'.

Type I: The most widely used index in the processing of satellite data is the Normalized Difference Vegetation Index (NDVI) defined as $[(\rho_N - \rho_R)/(\rho_N + \rho_R)]$, where ρ_N and ρ_R are spectral bidirectional reflectance factors (ratio of the radiance of a target surface to the radiance of a conservative, lambertian surface) at near-infrared and red wavelengths, respectively [11]. To obtain a continuous form let NDVI = ΔV, $\rho_N = \rho(\lambda + \Delta\lambda)$ and $\rho_R = \rho(\lambda)$. Note that

$$\rho(\lambda + \Delta\lambda) - \rho(\lambda) = \frac{d\rho}{d\lambda}\Delta\lambda + \Theta[(\Delta\lambda)^2] \tag{1}$$

$$\rho(\lambda + \Delta\lambda) + \rho(\lambda) = \frac{2}{\Delta\lambda}\int_{\lambda}^{\lambda+\Delta\lambda} d\lambda'\ \rho(\lambda') + \Theta[(\Delta\lambda)^2]. \tag{2}$$

Here $\Theta(\Delta\lambda^2)$ denotes error of order $\Delta\lambda^2$. In the limit $(\Delta\lambda \to 0)$

$$\frac{dV}{d\lambda} = \frac{d\rho}{d\lambda}\, k \tag{3}$$

where $k = [1/2\rho(\lambda)]$. The Soil Adjusted Vegetation Index, designed to minimize the soil effect in a vegetation signal [12], can be similarly expressed (3) with $k = (1+a)/[2\ \rho(\lambda) + a]$; a is a constant. The Simple Ratio (SR) is equivalent to NDVI because $NDVI$ = (SR − 1) / SR + 1) and therefore $k = [1/\rho(\lambda)]$.

A related class of indexes employs a weighted contrast in red/near-infrared reflectance to minimize soil effects. The continuous forms of these indexes (Weighted Difference-, Perpendicular- and Transformed Soil Adjusted-Vegetation Index) can also be expressed in a similar manner (Appendix A). Therefore, indexes containing a simple or weighted contrast can be grouped in $(k\ d\rho/d\lambda)$ (Fig. 1).

Type II: Vegetation indexes in this category are non-linear because they contain products of reflectance. For example, the Global Environment Monitoring Index (GEMI), designed to minimize atmospheric effects in Advanced Very High Resolution Radiometer data [16], can be shown (Appendix B) to conform to

$$\frac{dV}{d\lambda} = \frac{d\rho^2}{d\lambda}\, k \tag{4}$$

where $k = 2 / [2\ \backslash rho(\lambda) + 0.5]$. Another index in this category is the Greenness [17], defined as $\sum_{i=1}^{n} A_i\rho_i$. The evaluation of $dV/d\lambda$ in the limit $(\Delta\lambda \to 0)$ is straightforward (Appendix C)

$$\frac{dV}{d\lambda} \propto \frac{d\rho\rho^{\ell}}{d\lambda}\, k_j. \tag{5}$$

The derivative $d\rho^2/d\lambda$ is shown in Fig. 1.

Type III: The Atmospherically Resistant Vegetation Index, developed to minimize atmospheric effects in Moderate Resolution Imaging Spectrometer data [18], is defined as $[(\rho_N - \rho_{R,B})/(\rho_N + \rho_{R,B})]$, where $\rho_{R,B} = \rho_R - \gamma(\rho_B - \rho_R)$ and ρ_B is reflectance at blue wavelength ($\sim$0.45 μm). The continuous form of this index is (Appendix D)

$$\frac{d^2V}{d\lambda^2} = \frac{d^2\rho}{d\lambda^2}\, k \tag{6}$$

where $k = 1 / [2\ \backslash rho(\lambda)]$. The related Soil and Atmospherically Resistant Vegetation Index [18] can be similarly expressed (6) with $\$k = (1+a) / [2\ \rho(\lambda) + a]$. These indexes are therefore grouped in $(k\ d^2\rho/d\lambda^2)$ (Fig. 1).

III. The Spectral Derivative

The reflectance of a vegetated surface depends on the structural and optical properties of the vegetation and underlying soil. In the case of remote directional measurements, the directions of incident solar radiation and observation also determine surface reflectance. However, only the optical properties of vegetation and soil control the spectral dependence of surface reflectance [19]. Therefore, $\rho(\lambda) = F[\rho_S(\lambda), \omega_L(\lambda)]$, where ω_L is leaf albedo, ρ_S is soil hemispherical reflectance, F is canopy reflection function and ρ is bidirectional reflectance factor of the vegetated surface at wavelength λ.

Radiation incident on a leaf may be specularly reflected at the surface, the magnitude of which is usually assumed to be small. If this is not the case, ρ must be assumed to denote the diffuse reflectance of a canopy only. Radiant energy reaching the interior of a leaf can be absorbed by the pigments, water and other constituents. The principal mechanism of scattering, defined here as change in direction of photon travel, is due to refractive index discontinuities at cell wall-air interfaces. Radiation not absorbed inside a leaf emerges diffused on both sides of the leaf [20]. The leaf albedo ω_L is thus the sum of leaf hemispherical reflectance and transmittance.

The optical system of a leaf can be modelled as a pile of transparent plates. Each plate represents a hypothetical layer of leaf-interior of unit thickness [21]. The number of plates is independent of wavelength. The spectral dependence of leaf albedo is governed by the transmittance κ of a single such plate and the refractive index ν of the cell walls. The latter however is a weak function of wavelength and a constant value of $\sim$1.4 can be assumed [21]. Thus, $\omega_L(\lambda) = P[\kappa(\lambda)]$; P is the leaf albedo function.

Bare soil reflectance ρ_S is a function of soil moisture and physical and optical properties of the soil particles [22]. Of these, only the single scattering albedo of the particles ω_S depends on the wavelength and soil moisture content [23]. Therefore, $\rho_S(\lambda) = Q[\omega_S(\lambda)]$; Q is the soil reflection function.

In light of the above discussion, the spectral derivative can be expanded as

$$\frac{d\rho}{d\lambda} \approx \frac{\partial F}{\partial \rho_S}\frac{\partial Q}{\partial \omega_S}\frac{d\omega_S}{d\lambda} + \frac{\partial F}{\partial \omega_L}\frac{\partial P}{\partial \kappa}\frac{d\kappa}{d\lambda}. \tag{7}$$

The functions F, Q, and P describe radiative transfer in a canopy of leaves layered above a soil surface, a semi-infinite medium of soil particles and the interior of a leaf modelled as a pile of transparent plates, respectively. The governing equations of transfer are linear integro-differential equations [24]. The solutions can be expressed formally as a sum of exponential functions, that is, the photon count decays exponentially through successive absorption and scattering events in the media. The partial derivatives ($\partial F/\partial\rho_S$, $\partial F/\partial\omega_L$, $\partial Q/\partial\omega_S$ and $\partial P/\partial\kappa$) are therefore exponential functions—smooth and smaller in magnitude than the total

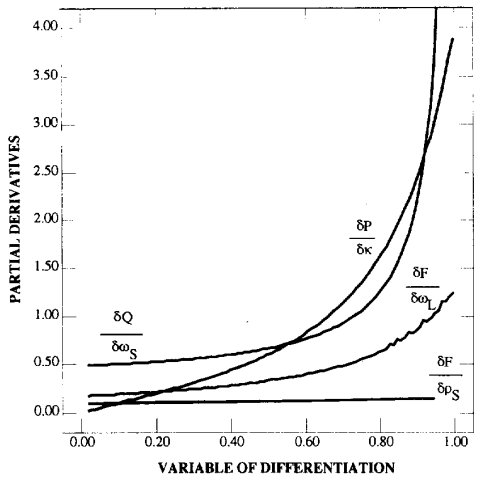

Fig. 2. Partial derivatives of the canopy reflection function F, soil reflection function Q and leaf albedo function P. ω_L is leaf albedo, ω_S is single scattering albedo of soil particles, κ is plate transmittance and ρ_S is soil hemispherical reflectance. Other parameters are as in Fig. 1.

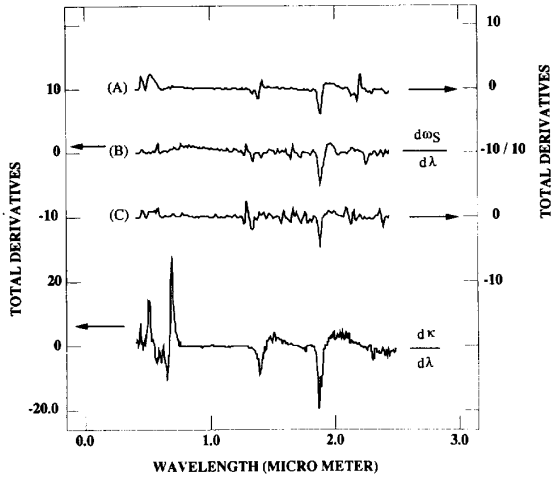

Fig. 3. The derivatives of plate transmittance κ and single scattering albedo of soil particles ω_S with respect to wavelength λ. ω_S data are for slightly moist clayey (A), peaty (B) and sandy (C) soils [23]. κ is for the soybean leaf discussed in [25].

derivatives ($d\omega_S/d\lambda$ & $d\kappa/d\lambda$) (Figs. 2 and 3). In particular, $|(\partial F/\partial \rho_S)(\partial Q/\partial \omega_S)| \ll |d\omega_S/d\lambda|$ and $|(\partial F/\partial \omega_L)(\partial P/\partial \kappa)| \ll |d\kappa/d\lambda|$. Hence

$$\frac{d\rho}{d\lambda} \propto \frac{d\omega_S}{d\lambda} + \frac{d\kappa}{d\lambda}. \tag{8}$$

This conclusion is also confirmed empirically (Fig. 4). Therefore, the symbolic representations $\rho(\lambda) = F[\rho_S(\lambda), \omega_L(\lambda)]$, $\rho_S(\lambda) = Q[\omega_S(\lambda)]$ and $\omega_L(\lambda) = P[\kappa(\lambda)]$ are assumed valid. A similar result for $d^2\rho/d\lambda^2$ can be shown (Appendix E).

Further insight can be gained if it is assumed that the leaf canopy is optically dense or that the soil is highly absorptive

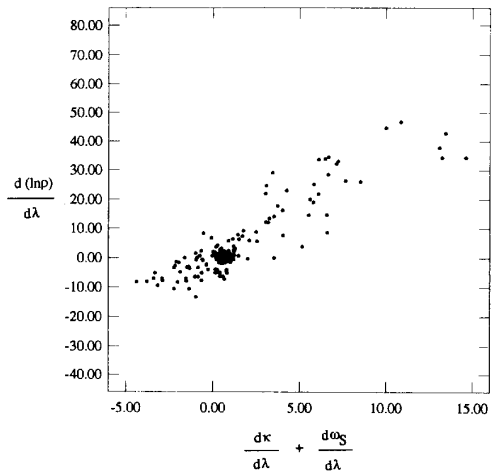

Fig. 4. The relationship between the spectral derivative of canopy reflectance and spectral derivatives of leaf and soil optical properties. Soil, leaf, and canopy spectra were measured in August 1989 at a natural grassland prairie (site 916) [30]. The soil reflectance spectrum was inverted using a model [23] to obtain the spectrum of soil-particle single scattering albedo $\omega_S(\lambda)$. The plate transmittance spectrum $\kappa(\lambda)$ was estimated by inverting a model [25] with measured leaf reflectance spectra. *Note that the ordinate is equivalent to the continuous form of NDVI.*

across the wavelength interval of interest, in which case

$$\frac{d\rho}{d\lambda} \propto \frac{d\kappa}{d\lambda}. \tag{9}$$

The reflectance spectrum $\rho(\lambda)$ in this instance is the convolution of plate transmittance spectrum $\kappa(\lambda)$ and a response function $R(\lambda)$; $\rho(\lambda) = R(\lambda) \star \kappa(\lambda)$ (7). The response function describes the effect of canopy architecture. The deconvolution of remotely sensed reflectance spectra with appropriate response functions is key to successful remote sensing.

IV. The Spectral Absorption Coefficient

The plate transmittance κ is equivalent to the spectral absorption coefficient α of an assembly of absorbers located in the plate

$$\kappa(\alpha) = (1-\alpha)\exp(-\alpha) + \alpha^2\, \mathrm{E}_1(\alpha) \tag{10}$$

where $\mathrm{E}_1(\alpha)$ is exponential integral of order one [21]. The key word here is "equivalence" because κ can be evaluated from α without requiring any other measurable intrinsic property of the leaf optical system. The absorption coefficient α is the product of absorber concentration per unit leaf area $\wp$ and absorber-specific absorption coefficient $\tilde{a}$ [25]. If N species are active at wavelength λ, $\alpha(\lambda) = \sum_i^N \wp_i \tilde{a}_i(\lambda)$.

The spectral derivative of an optically dense canopy in terms of the above is (Appendix F)

$$\frac{d\rho}{d\lambda} \equiv \frac{\partial P}{\partial \kappa}\left\{\frac{\partial F}{\partial \omega_L}\right\} \sum_{i=1}^{N} \mathrm{L}_i \wp_i\, \Psi(\alpha_i). \tag{11}$$

Here L_i is the total leaf area per unit ground area, over which the ith-absorber species is distributed. Consequently,

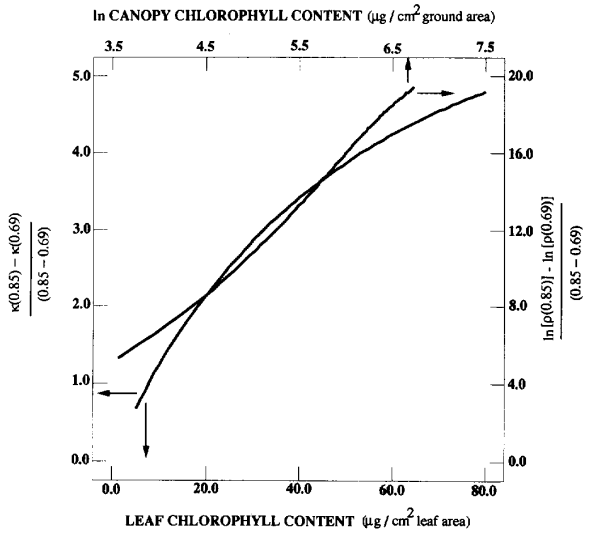

Fig. 5. The relationship between the discrete derivative of plate transmittance κ and soybean leaf chlorophyll content. A similar relationship at the canopy scale is also shown; ρ is modelled canopy reflectance [19]. Other parameters are as in Fig. 1.

$\mathrm{L}_i\wp_i$ denotes the concentration of the ith-absorber species per unit ground area. Therefore

$$\frac{d\rho}{d\lambda} \propto \sum_{i=1}^{N} \mathrm{L}_i\wp_i \propto \sum_{i=1}^{N} \mathrm{L}_i\wp_i\tilde{a}_i \tag{12}$$

that is, the spectral derivative is indicative of the abundance and activity of the absorbers pertaining to radiation absorption. In fact $d\rho/d\lambda = -dA/d\lambda$, where A is the fraction of incident radiant flux density absorbed by an optically dense canopy of horizontal lambertian leaves, because $\rho + A = 1$ from energy conservation. Therefore, sensing a surface remotely with measurements of scattered radiation is equivalent to inferring radiation absorption by the surface. This is the theoretical basis sought for satellite remote sensing of leaf biochemical constituents (Appendix G). The related forms $d^2\rho/d\lambda^2$ and $d\rho^2/d\lambda$ can be similarly interpreted. It is therefore concluded that spectral vegetation indexes are indicative of the abundance and activity of the absorbers in the leaves. The indexes saturate at sufficiently high values of $\mathrm{L}_i\wp_i$ (11).

V. Red/Near-Infrared Vegetation Indexes

The *in vivo* absorption spectra of chlorophylls a & b peak at about 0.69 μm and approach zero at 0.85 μm [25]. Following (9) and (12), $\Delta\kappa/\Delta\lambda$ and $\Delta\rho/\Delta\lambda$ evaluated at these wavelengths are indicative of chlorophyll abundance and energy absorption (Fig. 5) – a result confirmed experimentally [28]. The broad-band red/near-infrared vegetation indexes can be similarly understood. Chlorophyll abundance and energy absorption influence plant growth through photosynthesis. This may be the basis for the observed correlations between red/near-infrared indexes and vegetation amount [3], the fraction of absorbed photosynthetically active radiation [4], unstressed vegetation conductance and photosynthetic capacity [5], and seasonal atmospheric carbon dioxide variations [6].

VI. Appendix A

The Weighted Difference Vegetation Index is defined as $(\rho_N - a\rho_R)$, where a is a constant [13]. Let $V_W(\lambda + \Delta\lambda) = [\rho(\lambda + \Delta\lambda) - a\rho(\lambda)]$ and $V_W(\lambda) = [(1 - a)\rho(\lambda)]$. Thus $\Delta V_W/\Delta\lambda = \Delta\rho/\Delta\lambda$ and in the limit $(\Delta\lambda \to 0)$

$$\frac{dV_W}{d\lambda} = \frac{d\rho}{d\lambda}.. \tag{A1}$$

The related Perpendicular Vegetation Index is defined as $c(\rho_N - a\rho_R - b)$, where a, b and c are constants [14]. Let $V_P(\lambda+\Delta\lambda) = c[V_W(\lambda+\Delta\lambda)-b]$ and $V_P(\lambda) = c[V_W(\lambda)-b]$. Thus $\Delta V_P/\Delta\lambda = c\Delta\rho/\Delta\lambda$ and in the limit $(\Delta\lambda \to 0)$

$$\frac{dV_P}{d\lambda} = \frac{d\rho}{d\lambda}\, c. \tag{A2}$$

A recent index in this category is the Transformed Soil Adjusted Vegetation Index (TSAVI) defined as [15]

$$\mathrm{TSAVI} = \frac{a(\rho_N - a\rho_R - b)}{a\rho_N + \rho_R - c}. \tag{A3}$$

Let

$$V_T(\lambda + \Delta\lambda) = \frac{a[V_W(\lambda + \Delta\lambda) - b]}{a[\rho(\lambda + \Delta\lambda) + \rho(\lambda)] + (1 - a)\rho(\lambda) - c} \tag{A4}$$

and

$$V_T(\lambda) = \frac{a[V_W(\lambda) - b]}{a[2\rho(\lambda)] + (1 - a)\rho(\lambda) - c}. \tag{A5}$$

Therefore $\Delta V_T/\Delta\lambda = k\,\Delta\rho/\Delta\lambda$ and in the limit $(\Delta\lambda \to 0)$

$$\frac{dV_T}{d\lambda} = \frac{d\rho}{d\lambda}\, k \tag{A6}$$

where $k = a/[\ (1+a)\ \backslash rho(\lambda) - c]$ (2).

VII. Appendix B

The Global Environment Monitoring Index is a quadratic in η where

$$\eta = \frac{2(\rho_N^2 - \rho_R^2) + 1.5\rho_N + 0.5\rho_R}{\rho_N + \rho_R + 0.5}. \tag{B1}$$

Let η_o =4 $\rho(\lambda)/$ [2 $\rho(\lambda)$+0.5] and $\Delta V = (\eta - \eta_o)$. In the limit $(\Delta\lambda \to 0)$ (4) results with $k = 2$ / [2 $\rho(\lambda)$+ 0.5].

$$\frac{d\kappa}{d\lambda} = \sum_{i=1}^{N} \wp_i \left[\frac{d\tilde{a}_i}{d\lambda}[\exp(-\alpha_i)(\alpha_i - 2) + 2\alpha_i \mathrm{E}_1(\alpha_i)] - \tilde{a}_i \exp(-\alpha_i)\right] = \sum_{i=1}^{N} \wp_i \Psi(\alpha_i) \tag{F4}$$

VIII. Appendix C

The coefficients A_i can be estimated from wet soil (ρ^w), dry soil (ρ^d) and green vegetation (ρ^g) reflectance spectra following a procedure outlined in [17]. When those identities are introduced into the definition of Greenness, $\sum_{i=1}^{n} A_i\rho_i$, the continuous form $dV/d\lambda$ results in the limit ($\Delta\lambda \to 0$)

$$\frac{dV}{d\lambda} = k_1 \sum_i \frac{d\rho_i \rho_i^g}{d\lambda_i} - k_1 \sum_i \frac{d\rho_i \rho_i^s}{d\lambda_i} + k_2 \sum_i \frac{d\rho_i \rho_i^w}{d\lambda_i} - k_2 \sum_i \frac{d\rho_i \rho_i^d}{d\lambda_i} \quad \text{(C1)}$$

Here ρ^s is soil reflectance, $k_1 = 1/G$ and $k_2 = D/BG$ [B, D and G are defined in [17].

IX. Appendix D

Let $\rho_B = \rho(\lambda)$, $\rho_R = \rho(\lambda + \Delta\lambda)$, $\rho_N = \rho(\lambda + 2\Delta\lambda)$ and $\gamma = 1$ [18]. Then

$$(\rho_N - \rho_{R,B}) = \Delta\lambda \left[\frac{d\rho}{d\lambda}\bigg|_{\lambda+\Delta\lambda} - \frac{d\rho}{d\lambda}\bigg|_{\lambda} \right] + \Theta[(\Delta\lambda)^3] \quad \text{(D1)}$$

$$(\rho_N + \rho_{R,B}) = \left[\frac{2}{\Delta\lambda} \int_{\lambda+\Delta\lambda}^{\lambda+2\Delta\lambda} d\lambda' \, \rho(\lambda') + \Delta\lambda \frac{d\rho}{d\lambda}\bigg|_{\lambda} \right] + \Theta[(\Delta\lambda)^2]. \quad \text{(D2)}$$

Let ARVI $= \Delta^2 V$ and in the limit ($\Delta\lambda \to 0$) (6) results.

X. Appendix E

The second order spectral derivative

$$\frac{d^2\rho}{d\lambda^2} \approx \frac{d}{d\lambda}\left[\frac{\partial F}{\partial \rho_S} \frac{\partial Q}{\partial \omega_S} \frac{d\omega_S}{d\lambda} + \frac{\partial F}{\partial \omega_L} \frac{\partial P}{\partial \kappa} \frac{d\kappa}{d\lambda} \right] \quad \text{(E1)}$$

can be simplified to

$$\frac{d^2\rho}{d\lambda^2} \propto \frac{d^2\omega_S}{d\lambda^2} + \frac{d^2\kappa}{d\lambda^2} \quad \text{(E2)}$$

because $|d^2\omega_S/d\lambda^2|$ and $|d^2\kappa/d\lambda^2|$ are several orders of magnitude greater than the absolute values of $d\rho_S/d\lambda$, $d\omega_S/d\lambda$, $d\omega_L/d\lambda$, $d\kappa/d\lambda$, $(d\omega_S/d\lambda)^2$, $(d\kappa/d\lambda)^2$ and all the first and second order partial derivatives of F, Q, and P with respect to ρ_S, ω_S, ω_L, and κ.

XI. Appendix F

Consider the case of an optically dense canopy of Lambertian, horizontal leaves. The spectral derivative is (7)

$$\frac{d\rho}{d\lambda} = \frac{\partial F}{\partial \omega_L} \frac{\partial P}{\partial \kappa} \frac{d\kappa}{d\lambda} \quad \text{(F1)}$$

Canopy reflectance in this case is also lambertian. The canopy reflection function F can be expressed analytically [26] and the partial derivative $\partial F/\partial\omega_L$ can therefore be evaluated

$$\frac{\partial F}{\partial \omega_L} = \mathrm{L}\left[\frac{1}{B}\Phi^-(\rho_S, X) - \frac{A}{B}\Phi^+(1, V) \right] = \mathrm{L}\left\{ \frac{\partial F}{\partial \omega_L} \right\} \quad \text{(F2)}$$

$$\Phi^{\pm}(x,y) = \frac{\partial W}{\partial \omega_L}\left(Wxe_1 + \frac{x}{\mathrm{L}}e_2 \pm ye_1 \right) + \frac{1}{\mathrm{L}}\frac{\partial y}{\partial \omega_L}[\exp(\pm p) - \exp(\mp p)] \quad \text{(F3)}$$

where $e_1 = \exp(p) - \exp(-p)$, $e_2 = \exp(p) + \exp(-p)$, $p = W\mathrm{L}$, ρ_S is soil hemispherical reflectance and L is leaf area index [W, X and V are defined in [26]. The derivative $d\kappa/d\lambda$ is (10), (see (F4), shown at the bottom of the previous page) where $\alpha_i = \wp_i \tilde{a}_i$. Inserting (F2) and (F4) in (F1) results in (11).

XII. Appendix G

The apparent reflectance of a vegetated surface $\bar{\rho}$ measured at the top of a cloudless atmosphere is related to surface reflectance ρ as: $\bar{\rho}(\lambda) = T[\tau_a(\lambda), \omega_a(\lambda), g_a(\lambda), \rho(\lambda)]$. The anisotropy parameter g_a is a weak function of wavelength and can be assumed constant. The aerosol optical depth τ_a and single scattering albedo ω_a vary near-linearly between $0.4 - 2.2\mu m$ [27]. The function T describes radiative transfer in an aerosol atmosphere. Its partial derivatives are therefore exponential and smaller in magnitude than $|d^2\rho/d\lambda^2|$. Thus

$$\frac{d^2\bar{\rho}}{d\lambda^2} \propto \frac{d^2\rho}{d\lambda^2} \quad \text{(G1)}$$

that is, the apparent surface reflectance, absent of gaseous and molecular interactions, is proportional to the true surface reflectance.

Acknowledgment

This research was funded by the Terrestrial Ecology Program of NASA. Dr. Wickland provided much needed impetus to this topic. The contributions of Drs. Ganapol and Jacquemoud are acknowledged with gratitude.

References

[1] P. J. Sellers and D. S. Schimel, "Remote sensing of the land biosphere and biogeochemistry in the EOS era: Science priorities, methods and implementation — EOS land biosphere and biogeochemical cycles panels," *Global Planetary Change*, vol. 7, pp. 279-297, 1993.

[2] G. Asrar and D. J. Dokken, Eds., *EOS Reference Handbook*. Washington, DC: NASA, 1993.

[3] C. J. Tucker, "Red and photographic infrared linear combination for monitoring vegetation," *Remote Sensing Environ.*, vol. 8, pp. 127-150, 1979.

[4] G. Asrar, M. Fuchs, E. T. Kanemasu, and J. L. Hatfield, "Estimating absorbed photosynthetic radiation and leaf area index from spectral reflectance in wheat," *Agron. J.*, vol. 76, pp. 300-306, 1984.

[5] P. J. Sellers, J. A. Berry, G. J. Collatz, C. B. Field, and F. G. Hall, "Canopy reflectance, photosynthesis and transpiration, III. A reanalysis using improved leaf models and a new canopy integration scheme," *Remote Sensing Environ.*, vol. 42, pp. 187-216, 1992.

[6] C. J. Tucker, Y. Fung, C. D. Keeling, and R. H. Gammon, "Relationship between atmospheric CO_2 variations and a satellite-derived vegetation index," *Nature*, vol. 319, pp. 195-199, 1986.
[7] C. J. Tucker, J. R. G. Townshend, and T.E. Goff, "African land-cover classification using satellite data," *Sci.*, vol. 227, pp. 369-375, 1985.
[8] A. F. H. Goetz, G. Vane, J. Solomon, and B. N. Rock, "Imaging spectrometry for earth remote sensing," *Sci.*, vol. 228, pp. 1147-1153, 1985.
[9] C. A. Wessman, J. D. Aber, D. L. Peterson, and J. A. Melillo, "Remote sensing of canopy chemistry and nitrogen cycling in temperate forest ecosystems," *Nature*, vol. 335, pp. 154-156, 1988.
[10] B. N. Holben, "Characteristics of maximum value composite images for temporal AVHRR data," *Int. J. Remote. Sensing,* vol. 7, pp. 1417-1437, 1986.
[11] J. W. Rouse, R. H. Hass, J. A. Schell, and D. W. Deering, "Monitoring vegetation systems in the Great Plains with ERTS," in *3rd ERTS Symp.*, NASA SP-351, U.S. Gov. Printing Office, Washington, DC, vol. 1, pp. 309–317, 1973.
[12] A. R. Huete, "A soil adjusted vegetation index," *Remote Sensing Environ.*, vol. 25, pp. 295-309, 1988.
[13] J. G. P. W. Clevers, "The application of a weighted infrared-red vegetation index for estimating leaf area index by correcting for soil moisture," *Remote Sensing Environ.*, vol. 29, pp. 25-37, 1989.
[14] A. J. Richardson and C. L. Wiegand, "Distinguishing vegetation from soil background information," *Photogramm. Eng.*, vol. 43, pp. 1541-1552, 1977.
[15] F. Baret and G. Guyot, "Potentials and limits of vegetation indexes for LAI and APAR assessment," *Remote Sensing Environ.*, vol. 35, pp. 161-174, 1991.
[16] B. Pinty and M. M. Verstraete, "GEMI: A non-linear index to monitor global vegetation from satellites," *Vegetatio*, vol. 101, pp. 15-20, 1992.
[17] R. D. Jackson, "Spectral indexes in n-spaces," *Remote Sensing Environ.*, vol. 13, pp. 409-421, 1983.
[18] Y. J. Kaufman and D. Tanré, "Atmospherically resistant vegetation index (ARVI) for EOS-MODIS," *IEEE Trans. Geosci. Remote Sensing,* vol. 30, 261-270, 1992.
[19] R. B. Myneni, G. Asrar, and S. A. W. Gerstl, "Radiative transfer in three dimensional leaf canopies," *Trans. Theory Stat. Phys.*, vol. 19, pp. 205-250, 1990.
[20] L. Grant, "Diffuse and specular characteristics of leaf reflectance," *Remote Sensing Environ.*, vol. 22, pp. 309-322, 1987.
[21] W. A. Allen, H. W. Gausman, A. J. Richardson, and J.R. Thomas, "Interaction of isotropic light with a compact plant leaf," *J. Opt. Soc. Am.*, vol. 59, pp. 1376-1379, 1969.
[22] B. Pinty, M. M. Verstraete, and R. E. Dickinson, "A physical model for predicting bidirectional reflectances over bare soils," *Remote Sensing Environ.*, vol. 27, pp. 273-288, 1989.
[23] S. Jacquemoud, F. Baret, and J.F. Hanocq, "Modeling spectral and bidirectional soil reflectance," *Remote Sensing Environ.*, vol. 41, pp. 123-132, 1992.
[24] S. Chandrasekhar, *Radiative Transfer.* New York: Dover, 1960.
[25] S. Jacquemoud and F. Baret, "PROSPECT: A model of leaf optical properties spectra," *Remote Sensing Environ.*, vol. 34, pp. 75-91, 1990.
[26] J. A. den Dulk, "The interpretation of remote sensing, a feasibility study," PhD dissertation, Agricultural Univ. Wageningen, Netherlands, 1989, p. 145.
[27] D. Tanré, C. Deroo, P. Duhaut, M. Herman, and J. J. Morcrette,"Simulation of the satellite signal in the solar spectrum (5S)," Laboratoire d'Optique Atmosphérique, Université des Sciences et Techniques de Lille, 59655 Villeneuve d'Ascq Cédex, France, p. 83-84, 1987.
[28] C. Buschmann and E. Nagel, "*In vivo* spectroscopy and internal optics of leaves as basis for remote sensing of vegetation," *Int. J. Remote Sensing,* vol. 14, pp. 711-722, 1993.
[29] K. J. Ranson, L. L. Biehl, and C. S. T. Daughtry, "Soybean canopy modelling data set," LARS Tech. Rep. 071584, Purdue Univ., W. Lafayette, Indiana, 1984.
[30] P. J. Sellers, F. G. Hall, G. Asrar, D. E. Strebel, and R. E. Murphy, "An overview of the First International Satellite Land Surface Climatology Project (ISLSCP) Field Experiment (FIFE)," *J. Geophys. Res.*, vol. 97, pp. 18345-18372, 1992.

Ranga B. Myneni received the Ph.D. degree in biology from the University of Antwerp, Antwerp, Belgium, in 1985.

He was previously employed by Kansas State University, Manhattan, and Georg-August Universität Göttingen, Germany, prior to joining Goddard Space Flight Center as an employee of the University of Maryland, College Park. His research interests are radiation transport and remote sensing of vegetation.

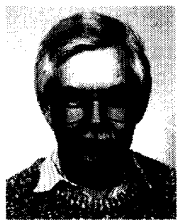

Forrest G. Hall received the B.S. degree from the University of Texas, Austin, and the M.S. and Ph.D. degrees in physics from the University of Houston, Houston, TX.

He is with NASA Goddard Spaceflight Center's Laboratory for Terrestrial Physics, where he currently serves as Project Manager for the Boreal Ecosystem-Atmosphere Study. During his 25-year NASA career, he has worked and published in the areas of spacecraft design, modeling planetary atmospheres, microwave remote sensing of sea surface wind fields, satellite calibration and atmospheric effects removal, image processing, mathematical pattern recognition, statistical sampling, global crop monitoring, climate/biosphere interactions, and forest ecosystem dynamics.

Piers J. Sellers received the B.Sc. degree in ecological science from the University of Edinburgh, Edinburgh, Scotland, and the Ph.D. degree in vegetation-atmospheric interactions from Leeds University, Leeds, UK, in 1976 and 1981, respectively.

Since 1982, he has bee working at the University of Maryland, College Park, and NASA Goddard Space Flight Center, on projects related to land biosphere-atmosphere interactions including integration of biosphere models and general circulation models, remote sensing of biophysical function, and design and execution of field experiments (FIFE and BOREAS). He is currently an interdisciplinary science investigator with the Earth Observing System and serves as the EOS-AM platform project scientist.

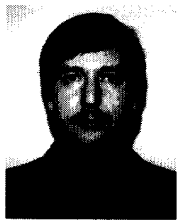

Alexander L. Marshak received the M.S. degree in applied mathematics from Tartu University, Estonia, and the Ph.D. degree in numerical analysis from the Siberian Branch of the Russian Academy of Sciences, Novosibirsk, Russia, in 1978 and 1983, respectively.

From 1978 to 1989, he was a Research Scientist at the Institute of Astrophysics and Atmospheric Physics, Tartu, Estonia. He was an Alexander von Humboldt Fellow from 1989 to 1991, and worked at the University of Göttingen, Germany. He is currently a Research Scientist in the Climate and Radiation Branch of NASA Goddard Space Flight Center. He has been actively involved in radiative transfer in atmosphere and vegetation since 1980. Since 1991, his research interests have been in nonlinear processes in geophysics and scale-invariant analysis of geophysical data. Currently, he is involved in theoretical cloud radiation studies in support of the Atmospheric Radiation Measurement program.